Grain-size effect on the deformation mechanisms of nanostructured copper processed by high-pressure torsion

X. Z. Liao, Y. H. Zhao, Y. T. Zhu, et al.

View Online   Export Citation

ARTICLES YOU MAY BE INTERESTED IN

Grain-size effect on the deformation mechanisms of nanostructured copper processed by high-pressure torsion

X. Z. Liao, Y. H. Zhao, and Y. T. Zhu[a]
Division of Materials Science and Technology, Los Alamos National Laboratory, Los Alamos, New Mexico 87545

R. Z. Valiev and D. V. Gunderov
Institute of Physics of Advanced Materials, Ufa State Aviation Technical University K. Marksa 12, Ufa 450000, Russian Federation

The unique nonuniform deformation characteristic of high-pressure torsion was used to produce nanostructures with systematically varying grain sizes in a copper disk, which allows us to study the grain-size effect on the deformation mechanisms in nanostructured copper using a single sample. The as-processed copper disk has 100–200 nm grains near its center and 10–20 nm grains at its periphery. High densities of full dislocations ($2 \times 10^{16}/m^2$) were distributed nonuniformly in large grains, implying that dislocation slip is the dominant deformation mechanism. With increasing dislocation density, the dislocations accumulated and rearranged, forming elongated nanodomains. The originally formed nanodomains remain almost the same crystalline orientation as their parent large grains. Further deformation occurred mainly through partial dislocation emissions from nanodomain boundaries, resulting in high density of nanotwins and stacking faults in the nanodomains. The elongated nanodomains finally transformed into equiaxed nanocrystalline grains with large-angle grain boundaries. The results suggest that grain boundary rotation and grain boundary sliding might play a significant role in the formation of large-angle grain boundaries in nanocrystalline grains. These experimental results show that different deformation mechanisms operate at different length scales and confirm unambiguously the deformation mechanisms of nanocrystalline grains predicted by molecular dynamic simulations. © *2004 American Institute of Physics.* [DOI: 10.1063/1.1757035]

I. INTRODUCTION

Nanostructured metals and alloys have demonstrated superior mechanical properties, such as excellent superplasticity,[1] high strength,[2–6] and, in a few cases, the combination of very high yield strengths and high ductility.[2,5,7] In contrast, there is always some trade-off between the strength and ductility in coarse-grained metals and alloys. The unique deformation mechanisms in nanostructured materials are believed responsible for the superior mechanical properties of the materials. Recently, tremendous effort has been made to understand the deformation mechanisms in nanostructured materials. For example, molecular dynamic simulations suggested that grain-boundary (GB) sliding plays a significant role at very fine grain sizes (e.g., 3–10 nm),[8] while partial dislocations emitted from GBs dominate the deformation at the grain sizes of several tens of nanometers.[9–11] Recent experimental observations on nanocrystalline Al and Cu have provided strong evidence of partial dislocation emission from GBs,[12,13] which subsequently form deformation twins and stacking faults. However, there has not been any report showing the systematic grain-size effect on deformation mechanisms in a relatively large grain-size spectrum from a single experiment. It is difficult for molecular dynamic simulations to study a system with rela-tively large grain sizes (e.g., around 100 nm) because of the limit in computing powers and resources. On the other hand, experimental studies involving multiple samples with different grains sizes may inadvertently introduce unintended factors that affect the deformation mechanism, because different processing parameters need to be employed to produce samples with different grain sizes. Therefore, it is desirable to produce nanostructures with systematically varying grain sizes in a single sample processed by a single set of parameters.

In this study, we employed the high-pressure torsion (HPT) technique to produce nanostructured copper with systematically varying grain sizes. During a typical HPT process, a sample disk is placed between two round tool-steel rods. The two rods apply a high pressure on the sample disk while rotating relative to each other. The severe plastic deformation produced by such a process will refine the grains of metal and alloy samples.[13–16] Due to the intrinsic nature of the HPT process, the sample disk does not deform uniformly,[15,17,18] which provides an excellent opportunity to study how different grain sizes (from submicrometers down to about 10 nm) affect the deformation mechanisms under similar deformation conditions. In this article, we carry out a careful transmission electron microscopy (TEM) investigation of the microstructures of a HPT-processed copper disk and report different deformation mechanisms in grains at different size ranges.

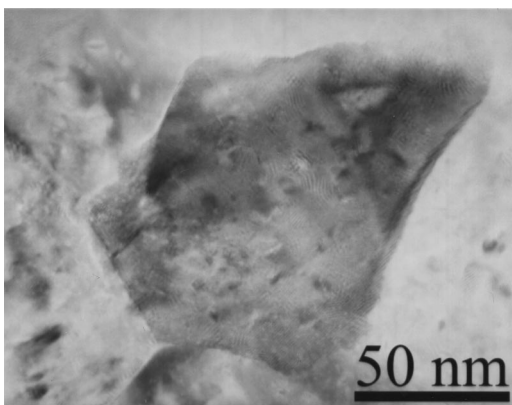---
[a]Electronic mail: yzhu@lanl.gov

FIG. 1. A typical bright-field TEM image of SMS grains.

II. EXPERIMENTAL PROCEDURES

A 99.99 wt % pure coarse-grained copper disk with a thickness of 0.5 mm and a diameter of 10 mm was processed into nanostructured copper via HPT for five revolutions under 7 GPa at room temperature and a quasistatic strain rate. Readers are referred to Refs. 15, 17, and 18 for detailed information on the HPT process. The samples for TEM investigation were prepared by mechanical grinding of the as-processed Cu disk to a thickness of about 10 μm and subsequent ion-milling. Special attention was paid to prevent any heating during the TEM sample preparation.

Conventional TEM investigation was carried out using a Philips CM30 microscope operated at 300 kV. High-resolution TEM (HREM) investigation was carried out using a JEOL 3000F microscope operated at 300 kV.

III. EXPERIMENTAL RESULTS

It is well known that for HPT deformation the true shear strain γ follows the relationship $\gamma = \ln(2\pi RN/L)$, where R is a radius, N is the rotation in turns, and L is the sample thickness.[15,18] This implies that HPT deformation in a disk will be nonuniform with the center of the disk being least deformed. Although experimental results have demonstrated increasing microstructural homogeneity with increasing applied pressure and rotation turns,[15,19] it is still expected that microstructures vary at the different parts of an HPT deformed sample. Indeed, TEM investigations show three distinct microstructures, which belong to three subsequent deformation stages, respectively, in the current sample: (i) submicron-sized (SMS) grains with the grain sizes ranging from about 100 nm to about 200 nm; (ii) elongated nanodomains, with the domain widths of around 10–20 nm, formed within the SMS grains; and (iii) equiaxed nanocrystalline grains with grain sizes around 10–20 nm. The different grain/domain sizes in one sample make it possible to systematically investigate the grain-size effect on the deformation behavior of nanostructured Cu under similar deformation conditions.

Figure 1 shows a typical bright-field image of SMS grains seen in the sample. Grains in this structure are usually at the size range of 100–200 nm. Although neighboring grains are all connected through large-angle GBs, detailed
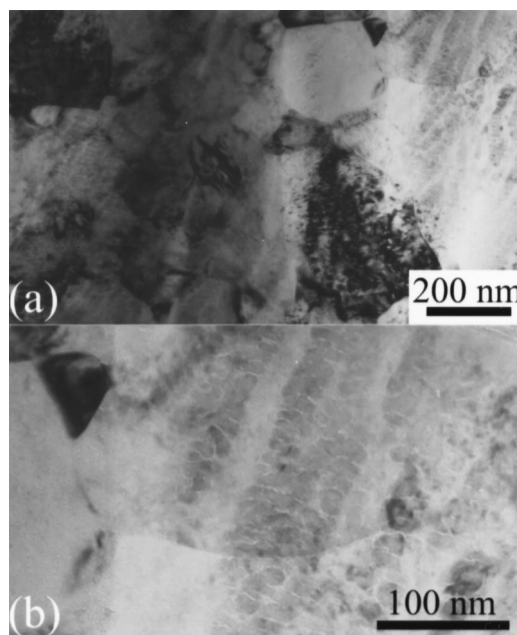

FIG. 2. (a) A typical low-magnification image of elongated nanodomains formed within SMS grains. (b) A magnified image of the upper right corner of (a).

investigation suggests that several neighboring grains usually form a domain in which the grain orientations are much closer to each other than the grain orientations in other domains. It is believed that grains within one domain were originally evolved from one coarse grain through a series of steps. Cellular subgrains were first formed with small-angle GBs followed by the subsequent small-angle to large-angle transformation of the GBs.[15,19–22] HREM examination of several grains suggests that the dislocation density in SMS grains is about $2 \times 10^{16}/m^2$ and the dislocations are not distributed uniformly. No twin was found in these SMS grains.

Figure 2 shows a typical bright-field image of elongated nanodomains formed within SMS grains. A structure similar to that seen in Fig. 1—grains with the size range of 100–200 nm—is seen at a low magnification in Fig. 2(a). However, at a high magnification in Fig. 2(b), it is seen that each SMS grain is further divided into a large number of elongated nanodomains (note: we name them "domains," not "grains" because neighboring nanodomains have almost the same orientation that contradicts the definition of "grains," see subsequent discussion) with widths of 10–20 nm. The elongation direction is the same for all nanodomains in different SMS grains, implying the direction was controlled by the sample torsion direction, not by the original grain orientation. The grain boundaries of the SMS grains remain clear and the nanodomains within each SMS grain have mainly the same orientation, which is clearly demonstrated from the same diffraction contrast within each SMS grain in Fig. 2(a), and will be further confirmed in Figs. 3 and 4 later.

As mentioned previously, dislocation density within each SMS grain is not uniform. As a result, some part of a SMS grain can be transformed into nanodomains, while the other part remains a large grain. A typical example is shown in a $\langle 110 \rangle$ HREM image in Fig. 3(a). It is interesting to note
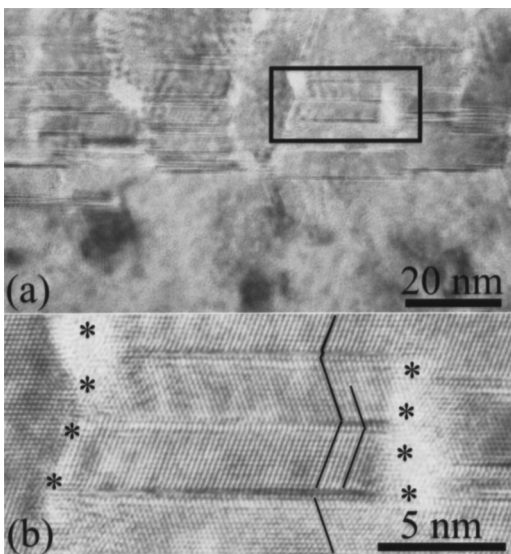
FIG. 3. (a) A ⟨110⟩ HREM image of a grain in which the upper part of the grain has been transferred into elongated nanodomains while the lower part still remains a SMS grain. (b) A magnified image of the part indicated by a black-rectangle in (a). The domain boundaries are highlighted using black asterisks. The {111} planes that form the twin relationship in the middle nanodomain are indicated using black lines.

FIG. 4. (a) A ⟨110⟩ HREM image of elongated nanodomains. The domain boundaries are highlighted using black asterisks. (b) Fourier transformation of (a). Two sets of lattice forming a twin relationship are indicated by two rectangles. (c) Inverse Fourier transformation using the (000) and two spots marked "C" in (b). Dislocation cores are marked with black "T" and their slip plane is indicated using a white straight line. A mark "A" indicates an area where dislocations are located within a nanodomain. (d) Inverse Fourier transformation using the (000) and two spots marked "D" in (b). Dislocation cores are marked with black "T."

that, while there is no deformation twin in the part that remains a large grain [see the lower part in Fig. 3(a)], nanotwins and stacking faults are seen everywhere in the nanodomain area in Fig. 3(a). To see the nanotwin HREM image more clearly, an area indicated by a black rectangle in Fig. 3(a) is enlarged and shown in Fig. 3(b). It is seen that the whole area is in an exact ⟨110⟩ zone-axis, although the area has been divided into a few nanodomains. The domain boundaries in Fig. 3(b) are highlighted using black asterisks. The {111} planes that form the twin relationship in the middle nanodomain are indicated using black lines. As shown in Fig. 3(b), the widths of twins in the middle and the right domains are different, and the twin mirror planes are not aligned with each other. This indicated that the twins were formed after the formation of those nanodomains, which is consistent with the fact that no twin is seen in large (SMS) grains.

In order to understand how elongated nanodomains formed within SMS grains, we analyze an HREM image, shown in Fig. 4(a), in which the domain boundaries are highlighted using black asterisks. The elongated nanodomains in Fig. 4(a) are all oriented along a ⟨110⟩ zone-axis. The Fourier transformation of Fig. 4(a) is shown in Fig. 4(b), indicating the existence of twins in Fig. 4(a). Inverse Fourier transformation using the central spot and the two spots marked with "C" in Fig. 4(b) gives a one-dimensional HREM image in Fig. 4(c). Figure 4(c) was analyzed carefully and the end of each half atomic plane, which is the core position of a dislocation line, is marked with black "T." The slip plane of the dislocation seen in Fig. 4(c) is indicated using a white straight line, which is roughly parallel to the nanodomain elongation direction. It is seen that, except for a few dislocations like those at the area marked with "A," most of the dislocations are located around the domain boundary areas,
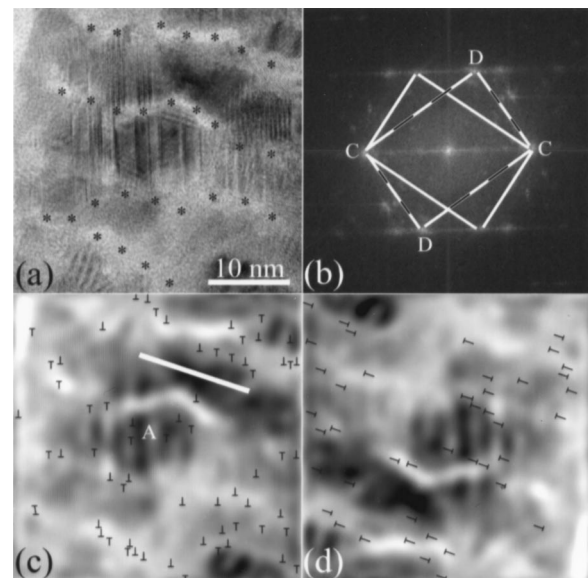
indicating that the domain boundaries were formed via dislocation accumulation. It is likely that the dislocations staying in area A are blocked by twin boundaries before they can reach the nearby domain boundaries. These dislocations blocked in elongated domains should have played an important role in converting the elongated domains into equiaxed grains at the last stage of microstructural evolution (see discussion of Fig. 5 later). Inverse Fourier transformation using the central spot and the two spots marked with "D" in Fig. 4(b) gives another one-dimensional HREM image in Fig. 4(d). The dislocation cores in Fig. 4(d) are also marked with a black "T." Similar to Fig. 4(c), most dislocations are distributed around domain boundary areas. However, unlike Fig. 4(c), in which most dislocations are 60°-type perfect dislocations, many dislocations in Fig. 4(d) are partial dislocations with a stacking fault behind each partial. It is important to note that the dislocation density in Fig. 4(c) is higher than that in Fig. 4(d), especially when the partial dislocations, which were formed after the formation of nanodomains [Fig. 4(d)], are excluded. This implies that the deformation along the white straight line direction shown in Fig. 4(c) (i.e., the nanodomain elongation direction) is more severe than other directions, and that the nanodomain elongation direction is probably close to the deformation torsion direction.

Figure 5 shows a typical bright-field image of equiaxed nanocrystalline grains, which are the finest grains observed in this sample. Morphology at this deformation stage is significantly different from the previous two stages: (1) no grain boundary of the parent SMS grains is seen; (2) most of the grains are equiaxed nanocrystalline grains; and (3) most
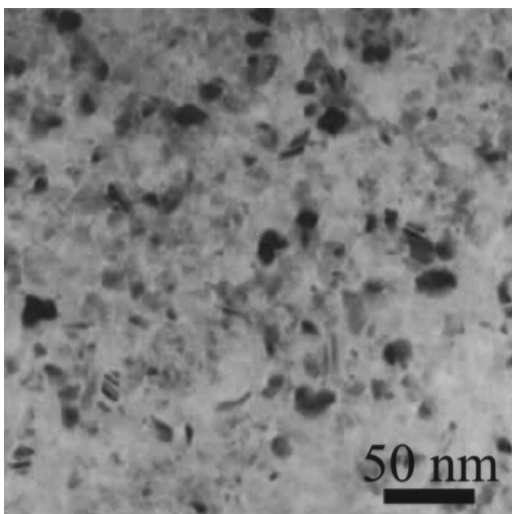
FIG. 5. A typical bright-field TEM image of equiaxed nanocrystalline grains.

grain boundaries are large-angle boundaries, as evidenced by the sharp diffraction contrast variation among neighboring equiaxed nanocrystalline grains in Fig. 5.

IV. DISCUSSION

Similar to other reported grain refinement process in severe plastic deformation,[15,19–22] SMS grains (see Fig. 1) were obtained through grain refinement that is caused by dislocation accumulation, interaction, tangling, and spatial rearrangement. Because neither stacking faults nor twins are seen in the SMS grains, the dislocations that were active during this deformation process are believed to be mainly full dislocations. The formation of elongated nanodomains is also through the slip of full dislocations. In fact, Meyers *et al.*[23] have reported that shock compression at 35 GPa produced abundant deformation twins in copper samples with grain sizes of 117 and 315 μm but virtually no twinning in a copper sample with a grain size of 9 μm, because the critical twinning stress is larger than the critical slip stress when a copper grain is smaller than a certain size. This result is consistent with what we have observed in this study.

The observation of twins in nanodomains violates the aforementioned trend on twining, implying that the grain-size effect on deformation twinning in coarse-grained copper (i.e., smaller grains are less likely to twin) does not apply to nanocrystalline copper. To explain this phenomenon, we notice that, in coarse-grained copper, twins are formed through the well-known pole mechanism. In contrast, detailed analysis of the twinning morphology in nanocrystalline copper grains has suggested that these twins were formed via partial dislocation emission from grain boundaries,[13] resulting in the invalidation of the trend on twinning[23] in nanocrystalline grains. Twinning has also been found prevalent in cryogenically ball-milled Al-Mg nanocrystalline grains when the grain sizes were reduced to smaller than 10 nm.[24] In fact, twinning in nanocrystalline grains through partial dislocation

emission from GBs has been predicted by molecular dynamic simulations[9–11] and has been recently confirmed by TEM observations of nanocrystalline Al.[12,25]

The process and mechanisms of partial dislocation emission from nanodomain boundaries are not well understood. Niewczas and Saada[26] recently proposed a partial dislocation source mechanism based on faulted dipoles. Such faulted dipoles could exist on the nanodomain boundaries and act as a source for partial dislocation emissions. More theoretical and experimental studies are needed to solve this issue.

Originally formed nanodomains are elongated and are of the same orientation as those formed from within a SMS grain. These elongated nanodomains will be further refined to equiaxed grains in the later deformation. Possible approaches include twinning and dislocation accumulation at the twin boundaries, like that shown in Fig. 4(c). Different from the situation in elongated nanodomains, the GBs of neighboring equiaxed nanocrystalline grains are usually large-angle boundaries. Given that dislocation activity has become difficult at this grain size range, grain rotation and grain boundary sliding might have played an important role for the formation of the large-angle GBs. Further experiments are needed to confirm this hypothesis. In fact, molecular dynamic simulations have predicted GB sliding in the deformation process of nanocrystalline materials.[8,27,28] An *in situ* TEM observation of deformation behavior of nanocrystalline gold thin films also confirmed that grain rotation and GB sliding play a significant role in a plastic deformation process of the nanostructured material.[29]

The discovery of the grain size-deformation mechanism relationship in this investigation is very important for designing material structures for optimal mechanical properties. It has been reported that GB sliding reduces the hardness and yield strength of nanostructured materials, resulting in a reverse Hall–Patch relationship.[8] On the other hand, Zhang *et al.*[30] recently reported that twinning in nanocrystalline stainless steel films significantly increases the hardness of the films because twin boundaries are very strong obstacles for dislocation movements. These results suggest that the grain/domain size before GB sliding occurs would be the strongest size in the copper sample in this investigation. However, how deformation mechanisms affect material ductility is still not clear, and more investigations are needed to understand this.

V. SUMMARY

A copper disk processed by HPT was investigated by HREM. The disk was not deformed uniformly, and three morphologies that correspond to three subsequent deformation stages were observed coexisting in the disk. The deformation mechanisms responsible for the three deformation stages were found to be different. SMS grains were obtained through grain refinement that is caused by dislocation accumulation, interaction, tangling, and spatial rearrangement. Elongated nanodomains were also obtained through a similar process. Partial dislocation emission from grain/domain boundaries is a major deformation mechanism in the elongated nanodomains, which subsequently resulted in the for-

mation of a high density of nanotwins and stacking faults. The elongated nanodomains later evolved into equiaxed nanocrystalline grains. Grain rotation and grain-boundary sliding might have played a significant role in the deformation process of the equiaxed nanocrystalline grains.

ACKNOWLEDGMENTS

[1] S. X. McFadden, R. S. Mishra, R. Z. Valiev, A. P. Zhilyaev, and A. K. Mukherjee, Nature (London) **398**, 684 (1999).

[2] R. Z. Valiev, I. V. Alexandrov, Y. T. Zhu, and T. C. Lowe, J. Mater. Res. **17**, 5 (2002).

[3] K. S. Kumar, S. Suresh, M. F. Chisholm, J. A. Horton, and P. Wang, Acta Mater. **51**, 387 (2003).

[4] D. Jia, Y. M. Wang, K. T. Ramesh, E. Ma, Y. T. Zhu, and R. Z. Valiev, Appl. Phys. Lett. **79**, 611 (2001).

[5] X. Zhang, H. Wang, R. O. Scattergood, J. Narayan, C. C. Koch, A. V. Sergueeva, and A. K. Mukherjee, Appl. Phys. Lett. **81**, 823 (2002).

[6] R. A. Masumura, P. M. Hazzledine, and C. S. Pande, Acta Mater. **46**, 4527 (1998).

[7] Y. M. Wang, M. W. Chen, F. H. Zhou, and E. Ma, Nature (London) **419**, 912 (2002).

[8] J. Schiøtz, F. D. Ditolla, and K. W. Jacobsen, Nature (London) **391**, 561 (1998).

[9] H. Van Swygenhoven, Science **296**, 66 (2002).

[10] V. Yamakov, D. Wolf, S. R. Phillpot, A. K. Mukherjee, and H. Gleiter, Nature Materials **1**, 1 (2002).

[11] V. Yamakov, D. Wolf, S. R. Phillpot, A. K. Mukherjee, and H. Gleiter, Acta Mater. **50**, 5005 (2002).

[12] X. Z. Liao, F. Zhou, E. J. Lavernia, S. G. Srinivasan, M. I. Baskes, D. W. He, and Y. T. Zhu, Appl. Phys. Lett. **83**, 632 (2003).

[13] X. Z. Liao, Y. H. Zhao, S. G. Srinivasan, Y. T. Zhu, R. Z. Valiev, and D. V. Gunderov, Appl. Phys. Lett. **84**, 592 (2004).

[14] A. P. Zhilyaev, J. Gubicza, G. Nurislamova, Á. Révész, S. Suriñach, M. D. Baró, and T. Ungár, Phys. Status Solidi A **198**, 263 (2003).

[15] H. G. Jiang, Y. T. Zhu, D. P. Butt, I. V. Alexandrov, and T. C. Lowe, Mater. Sci. Eng., A **290**, 128 (2000).

[16] V. V. Stolyarov, Y. T. Zhu, T. C. Lowe, and R. Z. Valiev, Nanostruct. Mater. **11**, 947 (1999).

[17] R. Z. Valiev, R. K. Islamgaliev, and I. V. Alexandrov, Prog. Mater. Sci. **45**, 103 (2000).

[18] A. P. Zhilyaev, G. V. Nurislamova, B. K. Kim, M. D. Baro, J. A. Szpunar, and T. G. Langdon, Acta Mater. **51**, 753 (2003).

[19] A. P. Zhilyaev, S. Lee, G. V. Nurislamova, R. Z. Valiev, and T. G. Langdon, Scr. Mater. **44**, 2753 (2001).

[20] I. V. Alexandrov, A. A. Dubravina, and H. S. Kim, Defect Diffus. Forum **208–209**, 229 (2002).

[21] N. Hansen and X. Huang, Acta Mater. **46**, 1827 (1998).

[22] Q. Liu, D. Juul Jensen, and N. Hansen, Acta Mater. **46**, 5819 (1998).

[23] M. A. Meyers, U. R. Andrade, and A. H. Chokshi, Metall. Mater. Trans. A **26**, 2881 (1995).

[24] X. Z. Liao, J. Y. Huang, Y. T. Zhu, F. Zhou, and E. J. Lavernia, Philos. Mag. **83**, 3065 (2003).

[25] X. Z. Liao, F. Zhou, E. J. Lavernia, D. W. He, and Y. T. Zhu, Appl. Phys. Lett. **83**, 5062 (2003).

[26] M. Niewczas and G. Saada, Philos. Mag. A **82**, 167 (2002).

[27] J. Schiøtz and K. W. Jacobsen, Science **301**, 1357 (2003).

[28] V. Yamakov, D. Wolf, S. R. Phillpot, A. K. Mukherjee, and H. Gleiter, Nature Materials **3**, 43 (2004).

[29] M. Ke, S. A. Hackney, W. W. Milligan, and E. C. Aifantis, Nanostruct. Mater. **5**, 689 (1995).

[30] X. Zhang, A. Misra, H. Wang, M. Nastasi, J. D. Embury, T. E. Mitchell, R. G. Hoagland, and J. P. Hirth, Appl. Phys. Lett. **84**, 1096 (2004).